



Originally published as:

Nowaczyk, N., Antonow, M. (1997): High-resolution magnetostratigraphy of four sediment cores from the Greenland Sea—I. Identification of the Mono Lake excursion, Laschamp and Biwa I/Jamaica geomagnetic polarity events. - *Geophysical Journal International*, 131, 2, pp. 310—324.

DOI: <http://doi.org/10.1111/j.1365-246X.1997.tb01224.x>

High-resolution magnetostratigraphy of four sediment cores from the Greenland Sea—I. Identification of the Mono Lake excursion, Laschamp and Biwa I/Jamaica geomagnetic polarity events

Norbert R. Nowaczyk,^{1*} and Martin Antonow²

¹ Fachbereich Geowissenschaften, Universität Bremen, Postfach 330440, D-28334 Bremen, Germany

² TU Bergakademie Freiberg, Institut für Geologie, Bernhard-von-Cotta-Str. 2, D-09596 Freiberg, Germany

Accepted 1997 June 17. Received 1997 June 17; in original form 1996 June 10

SUMMARY

High-resolution magnetostratigraphic analysis of three sediment cores from the base of the volcanic seamount Vesteris Banken in the Greenland Basin and one core from the Jan Mayen Fracture Zone revealed records of three pronounced geomagnetic events within the last 200 ka. Dating by stable carbon and oxygen isotope analysis, AMS¹⁴C measurements and biostratigraphic data (foraminifera abundances) yielded ages of 28–27 ka for the Mono Lake excursion, 37–33 ka for the Laschamp event, and 189–179 ka for the Biwa I event. In at least one of the cores the Laschamp event exhibits a full reversal of the local geomagnetic field vector. The same is true of the Biwa I event, documented in one of the cores.

Key words: Biwa I event, Brunhes Chron, Greenland Sea, Laschamp event, magnetostratigraphy, Mono Lake excursion.

INTRODUCTION

In this paper we report results relating to short-polarity events within the geomagnetic Brunhes Chron. Sediment cores recovered by R/V Polarstern from the Greenland Sea at about 73.5°N presented an opportunity to fill a gap in the database of these high-frequency features of the geomagnetic field as derived from sites further north and south. Magnetostratigraphic data from sediment cores recovered along a transect across the Kolbeinsey Ridge at 69.5°N (Bleil & Gard 1989), in the Fram Strait at 79°N (Nowaczyk 1991; Nowaczyk & Baumann 1992) and on the Yermak Plateau at 81°N (Løvlie *et al.* 1986) and 82°N (Nowaczyk *et al.* 1994) yielded consistent evidence that the Brunhes Chron of normal polarity has been interrupted by several short intervals of reversed polarity with a duration of up to 10 ka. The predominant lithogenic origin of the sediments results in fairly high intensities of the natural remanent magnetization (NRM), enabling a stepwise and complete demagnetization of the magnetostratigraphic samples with the remaining remanence still significantly higher than the noise level of the cryogenic magnetometers used for the measurements. Bioturbation in these sediments is fairly low or not observed over long sections of the recovered cores. The sediments investigated therefore

proved to be an ideal material to study geomagnetic excursions and polarity events as documented in the deposits of the Greenland Sea.

Sedimentological parameters, biostratigraphic data and, in particular, continuous high-resolution logging of the magnetic susceptibility performed on the cores investigated for this study permitted a detailed correlation of the recovered sediments. Analysis of stable isotopes, $\delta^{18}\text{O}$ and $\delta^{13}\text{C}$, and AMS¹⁴C (accelerator mass spectrometry) dating provided a sufficient time frame to reconstruct the geomagnetic field variations throughout the last *c.* 200 ka. The new high-resolution data support the results on the geomagnetic events already derived from sediments between 69.5°N and 82°N, and provide further detailed information on their palaeomagnetic signature, time of occurrence and duration.

GEOLOGICAL AND OCEANOGRAPHIC SETTINGS

The Greenland Sea basin structure is linked to major fracture zones and ridges (Vogt 1986). The surrounding morphological structures, for example the Greenland continental slope with its adjacent shelf and the Knipovich and Mohs ridges, are controlling factors of the oceanic circulation (Johannessen 1986). Plate tectonic spreading processes have led to the development of a complex bathymetry since the Palaeocene (Fig. 1). One of the results of basaltic volcanism is the genesis of the Vesteris Banken seamount, which rises up from the

* Now at: GeoForschungsZentrum Potsdam, Projektbereich 3.3, Laboratory for Paleo- and Rock Magnetism, Telegrafenberg, D-14473 Potsdam, Germany. E-mail: nowa@gfz.potsdam.de

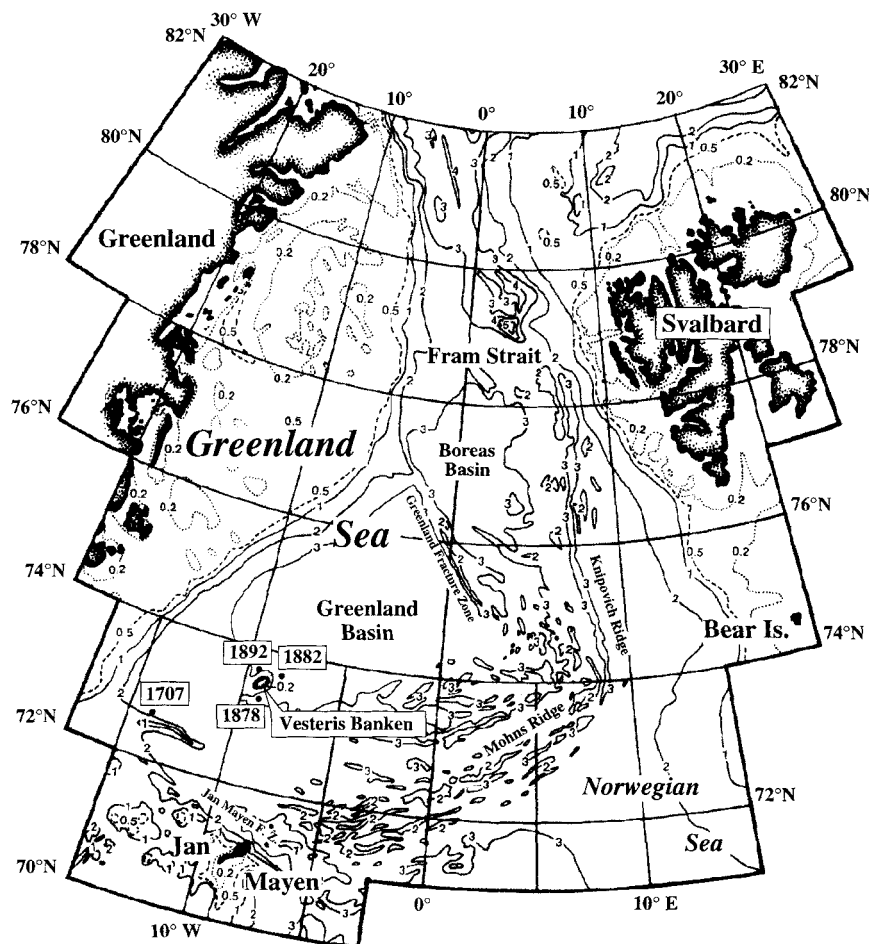


Figure 1. Bathymetry of the Greenland Sea and adjacent areas after Perry *et al.* (1986). Numbers around Vesteris Banken seamount indicate sites of sediment cores investigated in this study. Depth intervals are in thousands of metres.

Greenland abyssal plain to a water depth of only 133 m (Johnson & Campsie 1976). This is a unique morphological feature of the northern North Atlantic ocean floor and necessitates a discussion of the influence on the hydromechanic regime in the vicinity of such isolated barriers (Hogg 1973; Roberts *et al.* 1974; Antonow 1995).

The Greenland Sea represents an important mediator between the Arctic ocean and the northern North Atlantic. This area is remarkably sensitive to oceanographic and climatic changes due to the exchange and mixing of water masses from the Polar and Atlantic regions. The modern hydrography of the Greenland Sea is dominated by water masses of the Arctic domain. The influence of contrasting water masses from the Polar and Atlantic domains in the Greenland Sea has been variable since middle Pleistocene times. Frequently, the oceanic fronts in the central Greenland Sea area have been close together, allowing only a narrow Arctic domain to exist (Jünger 1994; Antonow 1995).

Greenland Sea sedimentation is mainly dominated by terrestrial sediment input. Large amounts of sediment-laden sea-ice are transported via the transpolar drift, mainly from the Eurasian shelves, across the North Pole to the Fram Strait, supplying fine-grained ice-rafted detritus (IRD) to the geosystem of the northern North Atlantic (Wollenburg 1993; Kassens *et al.* 1994). Another source of IRD is calving of glaciers from the Greenland, Scandinavian and Barents Sea ice sheets.

Within the Greenland Sea, IRD is distributed by the southerly directed East Greenland current and the anticyclonic Greenland Sea gyre, Jan-Mayen and Return Atlantic current circulations. IRD abundance in Pleistocene sediments documents the persistent climatic contrasts of severe polar conditions and iceberg melting in parts of the Greenland Sea and in the Fram Strait (Bischof 1990; Spielhagen 1991; Baumann *et al.* 1994; Goldschmidt 1994; Nam *et al.* 1995).

Planktic and/or benthic fossils are rare in Greenland Sea sediments during glacial highstands (Baumann 1990; Birgisdottir 1991; Struck 1992; Bauch 1993; Jünger 1994). The local abundance of coccolithophorids, however, documents uninterrupted biogenic sediment input during glacial conditions (Gard 1987, 1988; Gard & Backman 1990). Primary production was, of course, much higher during interglacial periods. The variations in calcium-carbonate content reflect strong climate-induced changes in the inflow of warm Atlantic surface-water masses and in palaeoproductivity (Baumann *et al.* 1993). The amounts of total organic carbon (0.2–0.3 weight per cent of bulk sediment) suggest 'normal' (hemi) pelagic sedimentation over large parts of the abyssal Greenland Sea (Jünger 1994; Antonow 1995).

CORE SITES AND MATERIALS

During two coring campaigns of the research ice-breaker R/V Polarstern, square-barrel Kastenlot corers (KAL) were

deployed in the Greenland Sea (Table 1). One KAL with an opening of 15×15 cm was recovered from the Jan Mayen Fracture Zone (site PS 1707; Cruise ARK V/3a) and three 30×30 cm KALs from the Greenland Basin around the base of the volcanic seamount Vesteris Banken (sites PS 1878, 1882

and 1892; Cruise ARK VII/1). All sediment cores are composed of greyish, greenish and brownish lithogenic hemipelagic muds with a grain-size range of clay to sandy silty clay. Sediments from the base of Vesteris Banken are interrupted by units of black coarse-grained ($> 63 \mu\text{m}$) to

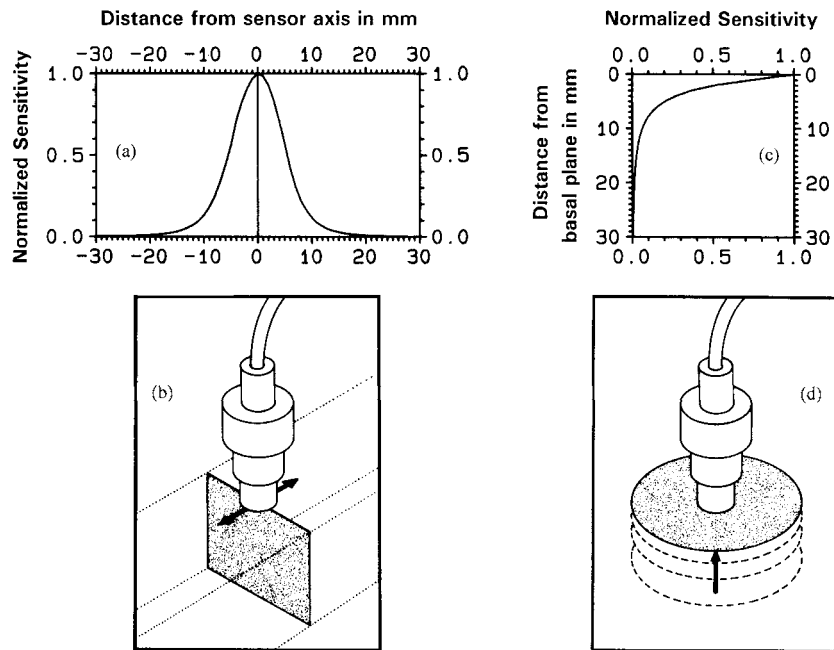


Figure 2. Spatial sensitivity of the Bartington MS2F sensor. The lateral sensitivity (a) was tested by moving a thin magnetite-covered plate along the base of the sensor according to (b). The vertical sensitivity (c) was tested by removing the plate according to (d).

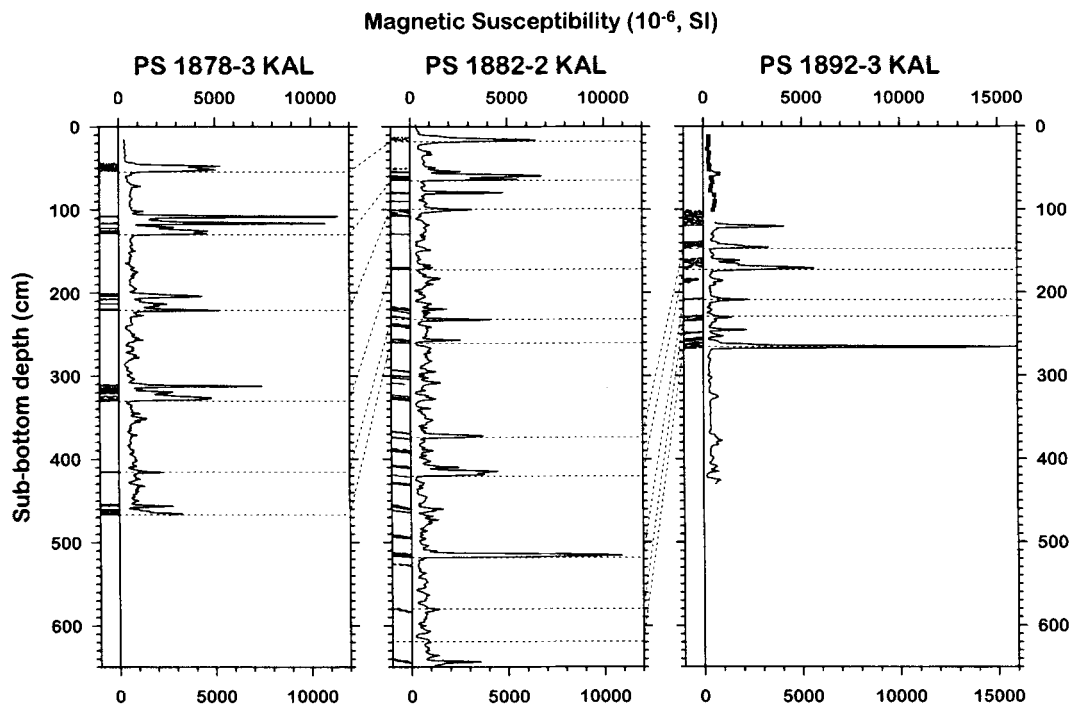


Figure 3. Correlation of sediment cores (dashed lines) recovered from the base of the volcanic Vesteris Banken seamount. High-resolution magnetic susceptibility logs derived from measurements on U-channels with a Bartington MS2F sensor at a spacing of 5 mm. Squares in the susceptibility log of PS 1892-3 KAL indicate where data were determined on discrete palaeomagnetic samples because of core disturbance. Black and grey stripes to the left of each log indicate the positions of volcanic ash layers.

Table 1. Location, water depth and length of sediment cores used in this study.

Core number	Latitude	Longitude	Water depth	Length
PS 1707-2 KAL*	72° 36.9' N	13° 48.4' W	2122 m	530 cm
PS 1878-3 KAL	73° 15.3' N	9° 00.7' W	3048 m	469 cm
PS 1882-2 KAL	73° 36.0' N	8° 19.3' W	3175 m	650 cm
PS 1892-3 KAL	73° 44.1' N	9° 41.2' W	3002 m	436 cm

KAL: square barrel Kastenlot corer, 30 × 30 cm; KAL*: 15 × 15 cm.

olive-green fine-grained (< 63 µm) volcanic (basaltic) ash layers. These ash layers are composed of glass and rock fragments together with some crystalline components. A detailed geochemical investigation has been performed by Haase, Hartmann & Wallrabe-Adams (1996). More detailed core descriptions of ARK VII/1 cores are given in Thiede & Hempel (1991) and Antonow (1995).

According to Nowaczyk & Baumann (1992), sampling for magnetostratigraphic and rock magnetic analysis was carried out using cubic plastic boxes (volume = 6.2 cm³) with a standard spacing from centre to centre of 5 cm. In addition, all four cores were subsampled using U-channels with an internal size of 28 × 28 mm and a length of 1100 mm with an overlap of about 200 mm.

MAGNETIC SUSCEPTIBILITY MEASUREMENTS

A Bartington MS2B sensor was used to determine the magnetic susceptibility κ of all palaeomagnetic samples at 460 Hz (low-frequency κ , κ_{LF}) and 4600 Hz (high-frequency κ , κ_{HF}). The

U-channel subcores were scanned with a Bartington MS2F sensor (operating frequency 580 Hz) in steps of 5 mm. The volume affected by the measuring field of the probe is very small. The sensor has a very narrow sensor characteristic along the core axis with a half-width of 12 mm (Figs 2a and b). The penetration of the measuring field was tested with a thin magnetite-covered disc according to Figs 2(c) and (d). The sediment can be looked upon as a continuous succession of such thin discs. Therefore, the value displayed by the susceptibility meter is proportional to the area below the curves in Figs 2(b) and (d). Because the response function in the vertical direction decreases very rapidly with distance from the sensor, it must be oriented strictly perpendicular to the sediment surface, completely touching it.

Prior to scanning, the sediment surface was cleaned and covered with a thin plastic foil to prevent the sensor from contamination. An empirically derived calibration factor of 16.1 was used to yield susceptibility multiples of 10⁻⁶ (SI). The drift of the probe was monitored by taking measurements every 10–20 cm at least 5 cm above the U-channel, so that the measuring field did not reach the core surface. The drift was interpolated linearly and subtracted from the logs.

Fig. 3 shows the correlation of the cores from the base of Vesteris Banken derived from high-resolution susceptibility logging of the U-channels. The logs are dominated by distinct peaks with extremely high susceptibility values of up to 16000 × 10⁻⁶ (SI). These peaks are related to the (basaltic) ash layers as indicated by the grey and black stripes to the left of each log in Fig. 3. The ash layers are situated within hemipelagic sediments where susceptibilities range from only 300 to 800 × 10⁻⁶ (SI). It can be assumed that due to the

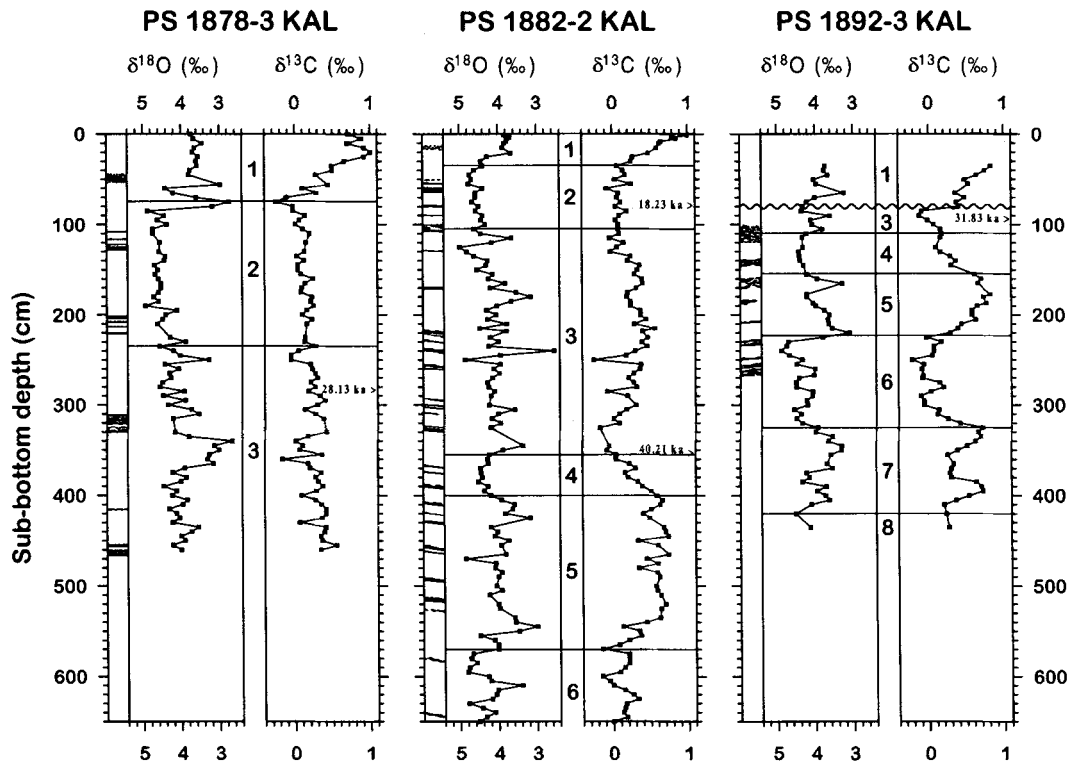


Figure 4. $\delta^{18}\text{O}$ and $\delta^{13}\text{C}$ records of *N. pachyderma* sin. from Vesteris Banken sediment cores. Numbers between the two records of each core denote oxygen isotope stages with their boundaries indicated by solid lines. AMS ^{14}C ages where indicated. Volcanic ash layers as in Fig. 3. The wavy line indicates a hiatus in core PS 1892-3 KAL.

directions of wind and water currents volcaniclastics ejected during an eruption will be deposited unevenly around Vesteris Banken. Therefore, the absolute amplitudes and the width of the peaks related to ash layers may vary within an order of magnitude. Nevertheless, the high data density of 200 measurements per metre and the spatial resolution of the MS2F sensor of 12 mm allows a very detailed peak-to-peak correlation of the susceptibility logs. For reasons of clarity, Fig. 3 shows only subsets of the correlation data, generally based on more than 50 depth levels in each core. The stable isotope data as well as biostratigraphic data, discussed in the next section, are included in the correlation scheme.

AGE MODEL FOR VESTERIS BANKEN SEDIMENTS ACCORDING TO AMS¹⁴C DATING, STABLE-ISOTOPE STRATIGRAPHY ($\delta^{18}\text{O}$, $\delta^{13}\text{C}$) AND BIOSTRATIGRAPHY

For AMS¹⁴C measurements, 1200–1300 specimens of the planktic foraminifera *Neogloboquadrina pachyderma* sin. were selected from the 125–250 μm grain-size fraction for each sample. The measurements were carried out at ETH Zurich (Switzerland) following the standard procedure described by Kromer *et al.* (1987). Determined ages were corrected according to Bard (1988), Bard *et al.* (1990) and Winn, Sarnthein & Erlenkeuser (1991). The results of the AMS¹⁴C measurements are listed in Table 2. The values are corrected for the marine reserve effect. It should be noted that the age of the sample from 350 cm sub-bottom depth (40.21 ka) in core PS 1882–2 KAL is probably out of the accuracy range of AMS dating

(about 40 ka). Therefore, this result is not used for further age modelling.

Stable isotope analysis was performed using 20–30 tests of *N. pachyderma* sin. (fraction 125–250 μm) per sample (Schiffelbein 1986). The material was prepared following the procedure of Duplessy (1978) and Ganssen (1983). The isotope ratios $\delta^{18}\text{O}$ and $\delta^{13}\text{C}$ were determined using a Finnigan MAT 251 mass-spectrometer at the C-14 Laboratory of the Christian-Albrechts-University of Kiel, Germany. The results are related to the PDB standard (Craig 1957; Craig & Gordon 1965). The deviation interval of measurements using very small amounts of sample (about 20 μg) ranges up to 0.09 ‰ for $\delta^{18}\text{O}$ values and up to 0.04 ‰ for the $\delta^{13}\text{C}$ measurements (H. Erlenkeuser, personal communication, 1994). The ratios of the stable isotopes $\delta^{18}\text{O}$ and $\delta^{13}\text{C}$ of the sediment cores from the Vesteris Banken area presented in Fig. 4 together with the AMS¹⁴C ages are typical of Middle/Late Pleistocene to Holocene values of the Norwegian–Greenland Sea. Comparisons with well-known patterns of $\delta^{18}\text{O}$ and $\delta^{13}\text{C}$ curves (Shackleton & Opdyke 1973, 1976; Imbrie *et al.* 1984; Martinson *et al.* 1987), as well as with more recent results from additional sites in the Norwegian–Greenland Sea (Vogelsang 1990; Sarnthein *et al.* 1992; Weinelt 1993; Jünger 1994), resulted in an oxygen isotope stratigraphy and the correlation of these three sediment cores (Antonow 1995).

The biogenic components from the coarse-grained fraction (125–500 μm) were counted in order to determine general trends in sedimentological variations. As a representative result the abundance patterns of the benthic foraminifera *Pyrgo* sp. and *Cibicoides wuellerstorfi* are displayed in Fig. 5. A

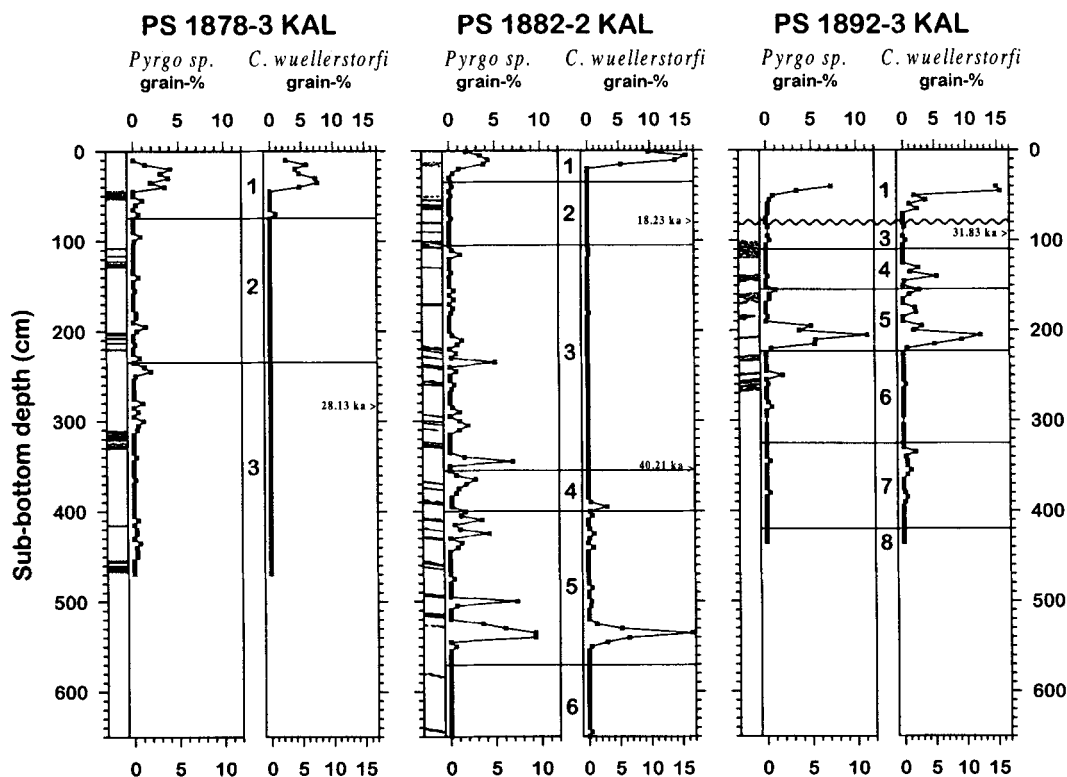


Figure 5. Abundance patterns of benthic foraminifera expressed by grain per cent of *Pyrgo* sp. and *Cibicoides wuellerstorfi* counted from the grain-size fraction 125–500 μm . Volcanic ash layers as in Fig. 3 and oxygen isotope stages as in Fig. 4.

Table 2. AMS¹⁴C ages of sediment samples from Vesteris Banken.

Core number	Sub-bottom depth (cm)	¹⁴ C age (ka)	¹⁴ C age corrected (ka)	Standard deviation 1σ (ka)
PS 1878-3 KAL	280	28.530	28.130	0.300
PS 1882-2 KAL	75	18.630	18.230	0.160
PS 1882-2 KAL	350	40.610	40.210	1.020
PS 1892-3 KAL	90	32.230	31.830	0.480

more detailed presentation of the biostratigraphic and sedimentological results is given in Antonow (1995).

The synthesis of magnetic susceptibility data, AMS¹⁴C ages, δ¹⁸O and δ¹³C stratigraphy and foraminifera abundance patterns facilitated the evaluation of the age model for the cores from Vesteris Banken, as shown in Table 3, and the correlation and assignment of oxygen isotope stage boundaries, as shown in Figs 3–5. Based on this age model, sedimentation rates for isotope stages 1–3 at site PS 1878 (about 10 cm ka⁻¹ on average) are twice as high as at site PS 1882 for the corresponding time interval. Although the Holocene deposits at site PS 1892 are also as thick as at site PS 1878, the younger glacial period (stages 2 and 3) is completely missing or documented by a much thinner sediment succession than at the other sites, as can be seen in particular from the biostratigraphic and isotope data (Figs 4 and 5). In general, sedimentation rates for isotope stages 4–6 at site PS 1892 (2.2 cm ka⁻¹) are lower than at site PS 1882 (5.5 cm ka⁻¹). The oldest sediments, reaching back to isotope stage 8, were recovered in the base of core PS 1892-3 KAL, from the site with the lowest sedimentation rates around Vesteris Banken.

The highly variable sedimentation rates around the Vesteris Banken seamount are obviously a result of the intraplate seamount itself. Such an isolated feature situated near the middle of the Greenland Basin acts as a barrier against moving water masses and results in a local distortion of the main water-current regime with a partly upwelling circulation pattern (Roden 1987) and significantly varying current velocities. Enhanced sedimentation is thus linked to decreased current velocities, whereas increased current velocities result in a reduced sedimentation or even erosion.

MAGNETOSTRATIGRAPHIC RECORDS

Measurements of the natural remanent magnetization (NRM) were mainly carried out at the Fachbereich Geowissenschaften (Department of Geoscience), University of Bremen, Germany, using a three-axis cryogenic magnetometer (Cryogenics Consultants, Model GM400). This instrument is based on AC-SQUIDS (Superconducting Quantum Interference Device) with a noise level of 10⁻⁵ A m⁻¹ maximum. Demagnetization of core PS 1707-2 KAL* was performed with a single-axis alternating-field (AF) demagnetizer, Schoenstedt GSD-1 (maximum AF amplitude 100 mT). A 2G Enterprises 600 degausser (maximum AF amplitude 270 mT) was used for cores PS 1878-3 KAL and PS 1882-2 KAL. For further details see Nowaczyk & Baumann (1992) and Nowaczyk *et al.* (1994). Finally, core PS 1892-3 KAL was processed at the Laboratory for Paleo- and Rock Magnetism of the GeoForschungsZentrum (GFZ) Potsdam, Germany, with a 2G Enterprises 755 SRM (Superconducting Rock Magnetometer) based on DC SQUIDS with a noise level of not more than 10⁻⁶ A m⁻¹. The magnetometer with an access diameter of 42 mm is equipped

Table 3. Age models for the three core sites around Vesteris Banken. Asterisks indicate AMS¹⁴C ages from Table 2.

Age (ka)	Sub-bottom depth (cm)		
	1878	1882	1892
0.00	0	0	30
6.50	35	7	55
9.00	56	21	65
12.05	75	35	85
15.00	90	45	
17.00	105	52	
17.50	130	65	
18.23	145	*75	
21.50	195	93	
22.50	201	98	
23.40	223	104	
24.11	235	110	85
27.00	255	145	
28.00	275	155	
28.13	*280	160	
28.80	286	163	
29.50	310	168	
30.00	330	172	
30.84	340	178	
31.83			*90
32.50	350	182	
35.00	367	198	
36.50	383	209	
37.50	390	215	
38.40	425	232	
39.70	432	242	
42.80	454	255	
43.80	469	260	
45.00		270	
59.00		355	112
68.00		375	147
73.91		400	155
79.25		410	160
90.95		435	177
99.38		465	190
129.84		570	223
135.10		590	240
139.00		607	252
152.58		630	280
175.05			290
179.00			300
189.61			325
193.07			345
200.57			360
215.54			370
224.89			380
240.19			405
244.18			420

with a long-core handler for U-channels with a maximum length of 150 cm, also usable for eight discrete samples at a spacing of 20 cm, and an in-line three-axis degausser (maximum AF amplitude 150 mT).

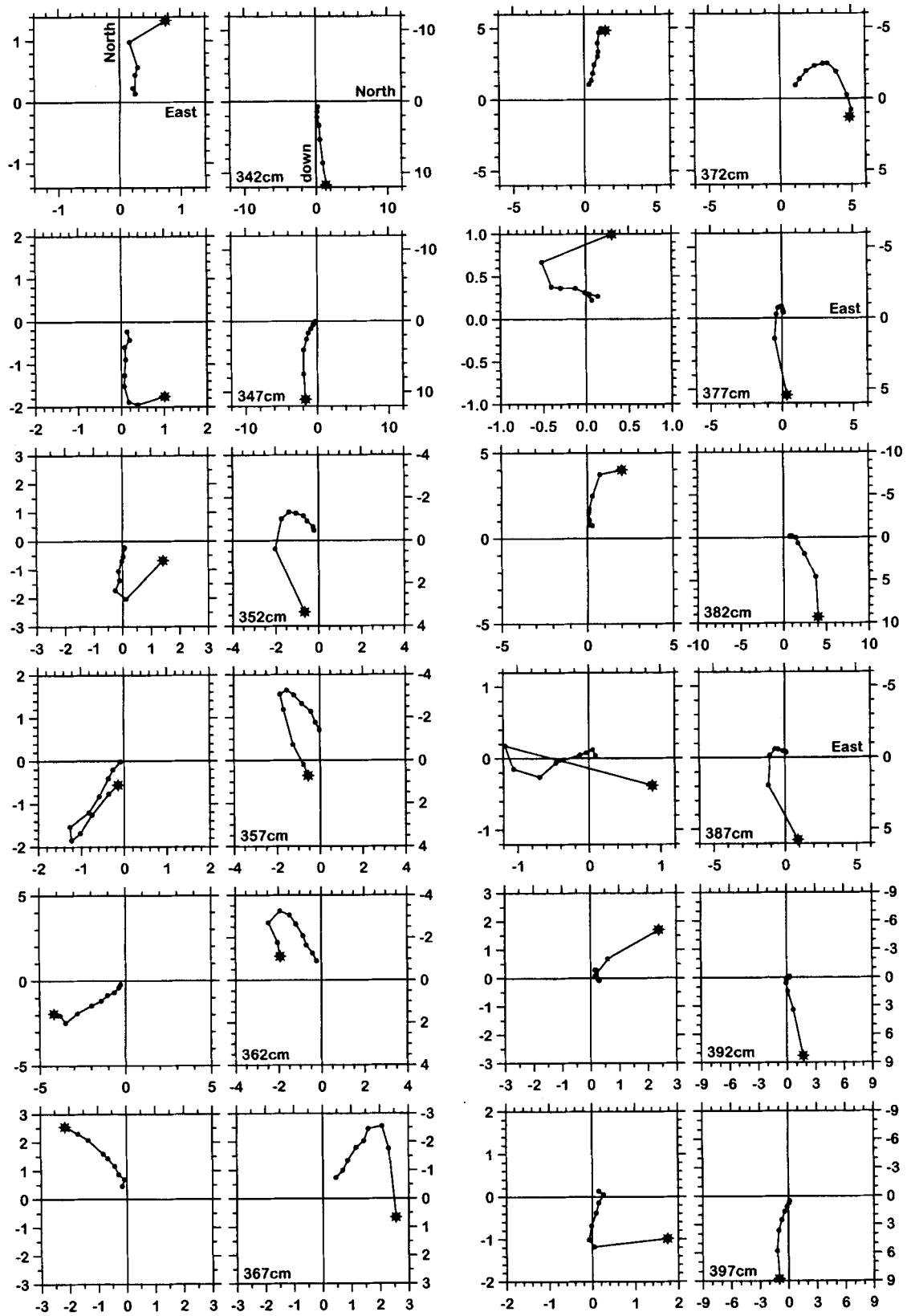


Figure 6. Orthogonal projections (Zijderveld diagrams) of 12 successive samples of core PS 1707-2 KAL* from the Jan Mayen Fracture Zone documenting the Laschamp geomagnetic polarity event. The left diagrams all display the horizontal magnetization components, whereas the right diagrams mainly display the vertical component versus the north/south component, or east/west component where indicated. The asterisk in each curve denotes the NRM measurement. The data are displayed in geographic coordinates (see text) and axis scaling is in mA m^{-1} .

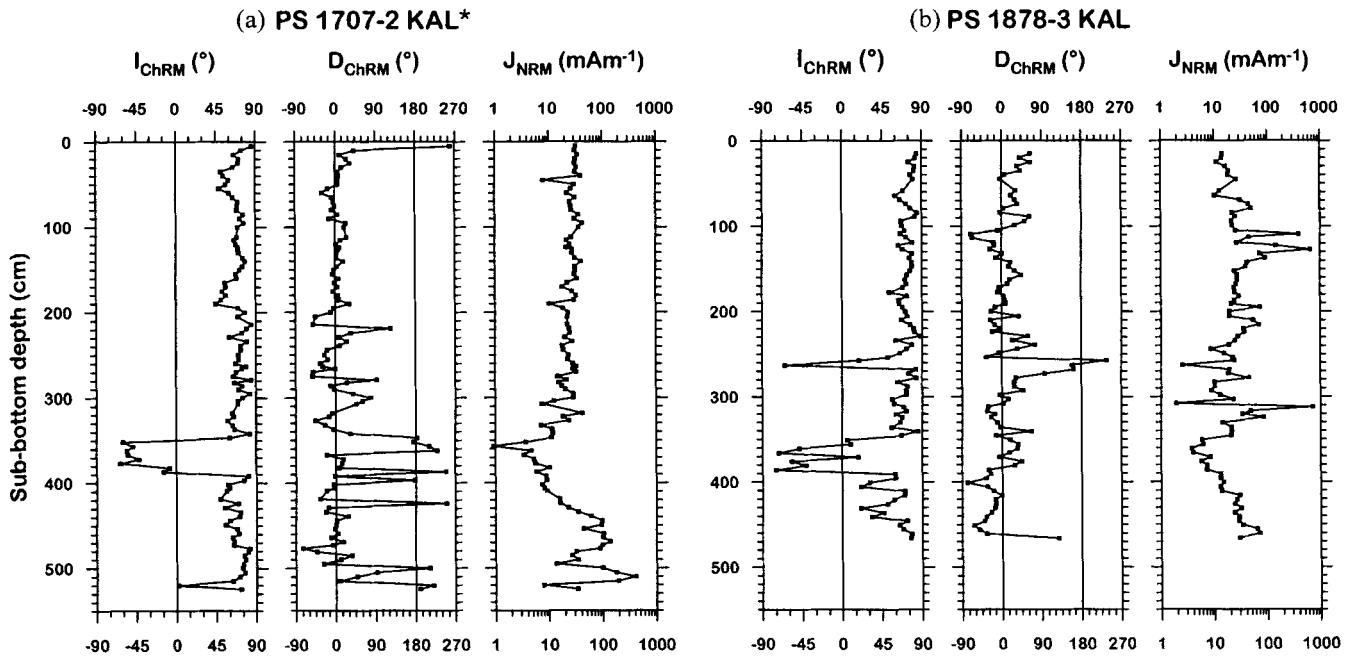


Figure 7. Magnetostratigraphic results of (a) core PS 1707-2 KAL*, Jan Mayen Fracture Zone, and (b) core PS 1878-3 KAL, Vesteris Banken seamount, Greenland Sea: downcore variations of ChRM inclination, ChRM declination and NRM intensity.

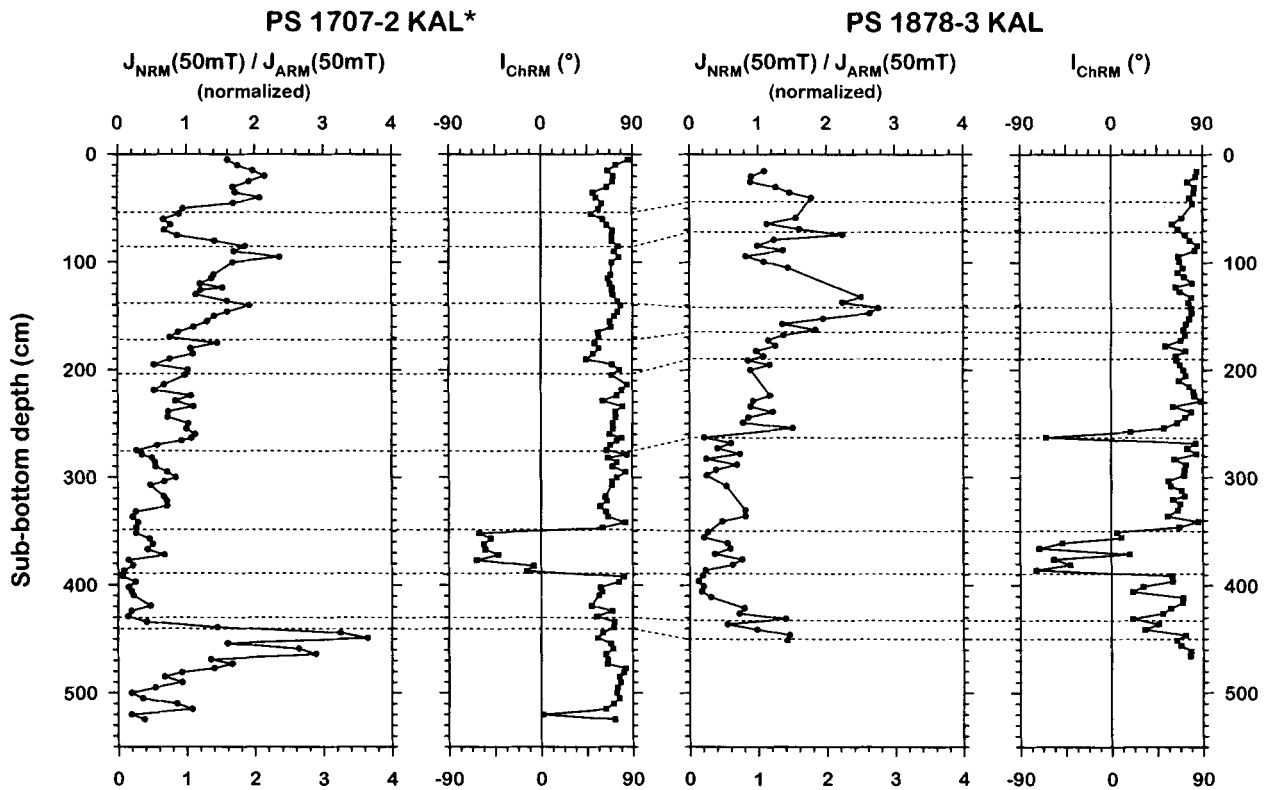


Figure 8. Correlation of core PS 1707-2 KAL* from the Jan Mayen Fracture Zone with core PS 1878-3 KAL from the base of Vesteris Banken using ChRM inclinations and the normalized relative palaeointensity records approximated by the ratio of NRM and ARM intensity after demagnetization with 50 mT.

NRM intensities of the cores investigated are in the range 10^{-2} – 10^{-1} A m⁻¹ for all four cores, with some samples reaching almost 1 A m⁻¹, associated with basaltic ash layers in Vesteris Banken sediments. After removal of viscous overprints, the quality criteria of Nowaczyk & Baumann (1992) were used to verify the stable direction of the characteristic remanent magnetization (ChRM):

- (1) monotonic decay of remanent magnetization with progressive AF demagnetization;
- (2) close clustering of the resultant vectors;
- (3) clustering of the difference vectors in the same direction as the resultant vectors;

which is equivalent to a decrease of the orthogonal vector components along straight lines through the origin of the Zijdeveld diagrams. The ChRM direction was calculated by averaging successive demagnetization steps with parallel resultant and difference vectors as well as by principle component analysis (Kirschvink 1980). The declinations of all normal-polarity samples ($I_{\text{ChRM}} > 45^\circ$) of a core were averaged as an approximation of the core's azimuthal orientation in order to interpret the recorded geomagnetic field variations with respect to geographic coordinates.

The demagnetization results processed in this way are now discussed with 12 successive samples of core PS 1707–2 KAL* (Fig. 6) from the Jan Mayen Fracture Zone. These samples, like all others from this core, were demagnetized in steps of 10, 20, 30, 40, 50, 65, 80 and 95 mT, some of them with additional steps of 2 and 5 mT. They document a geomagnetic polarity event within oxygen isotope stage 3, identified as the Laschamp event (Bonhommet & Babkine 1967). The Zijdeveld diagrams of Fig. 6 are plotted in absolute intensities (mA m⁻¹) in order to demonstrate that the magnetization is clearly above the maximum noise level of the magnetometers (10^{-5} A m⁻¹), even at the maximum demagnetization level of 95 mT. In all 12 samples a steep normal-polarity overprint was first removed. After the application of AF levels of 30–50 mT, stable directions of different varieties are isolated: negative inclinations associated with northerly (372 cm), as well as westerly (357, 362 and 367 cm) and southerly (347 and 352 cm), declinations. The last two samples can be looked upon as fully reversed, whereas the other samples mentioned previously represent more intermediate field directions. Sample 397 cm, with a stable steep positive inclination but southerly declination, also represents an intermediate field direction.

The magnetostratigraphic results, downcore variations of ChRM inclination and corrected declination together with the NRM intensity of core PS 1707–2 KAL* are illustrated in Fig. 7(a), showing the pronounced polarity reversal of the Laschamp event in the lower part of the core. A fairly similar magnetostratigraphic record was obtained for core PS 1878–3 KAL from the base of Vesteris Banken (Fig. 7b). Again, the Laschamp event with a pronounced inclination anomaly (350–390 cm) is documented in the ChRM inclination log but with northerly declinations ($\approx 0^\circ$) only. In addition, further upcore at 260 cm, a younger short excursion is documented. One sample shows both a negative ChRM inclination and a southerly ChRM declination ($\approx 180^\circ$), and the next four younger samples define a clear trend over shallow to steep normal inclinations. At least one sample directly above and below the fully reversed sample also shows a declination strongly deviating from the majority of the (normal-polarity) samples. This

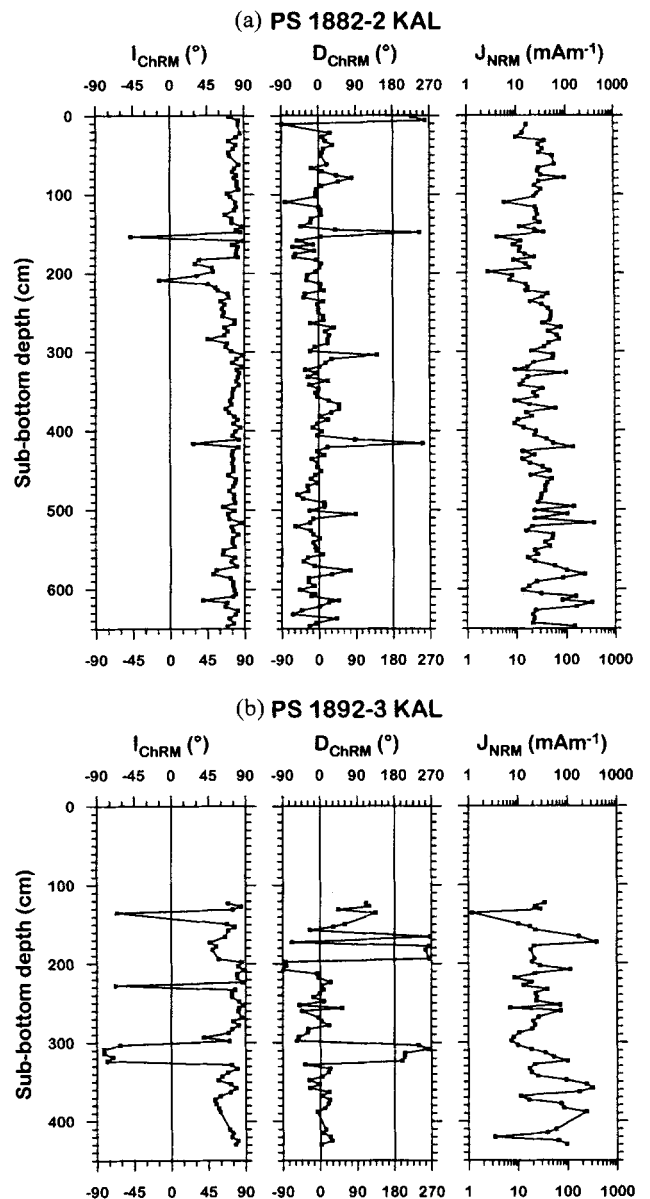


Figure 9. Magnetostratigraphic results of (a) core PS 1882–2 KAL and (b) core PS 1892–3 KAL, Vesteris Banken seamount, Greenland Sea: downcore variations of ChRM inclination, ChRM declination and NRM intensity.

excursion can be related to the Mono Lake event (Denham & Cox 1971) because it is located 20 cm above an AMS¹⁴C dating which assigns an age of 28.13 ka to the sub-bottom depth of 280 cm (Table 2).

Correlation and dating of core PS 1707–2 KAL* from the Jan Mayen Fracture Zone with core PS 1878–3 KAL from the base of Vesteris Banken could be achieved by using the ChRM inclination and the relative palaeointensity records approximated by the ratio $J_{\text{NRM}}(50 \text{ mT})/J_{\text{ARM}}(50 \text{ mT})$ (Fig. 8). The high-resolution magnetic susceptibility logs derived from U-channels were also used in order to refine this correlation. For the approximated palaeointensity record of core PS 1878–3 KAL all samples taken from ash layers were left out so that the record is based only on data from hemipelagic muds with quite reasonably constant rock magnetic parameters

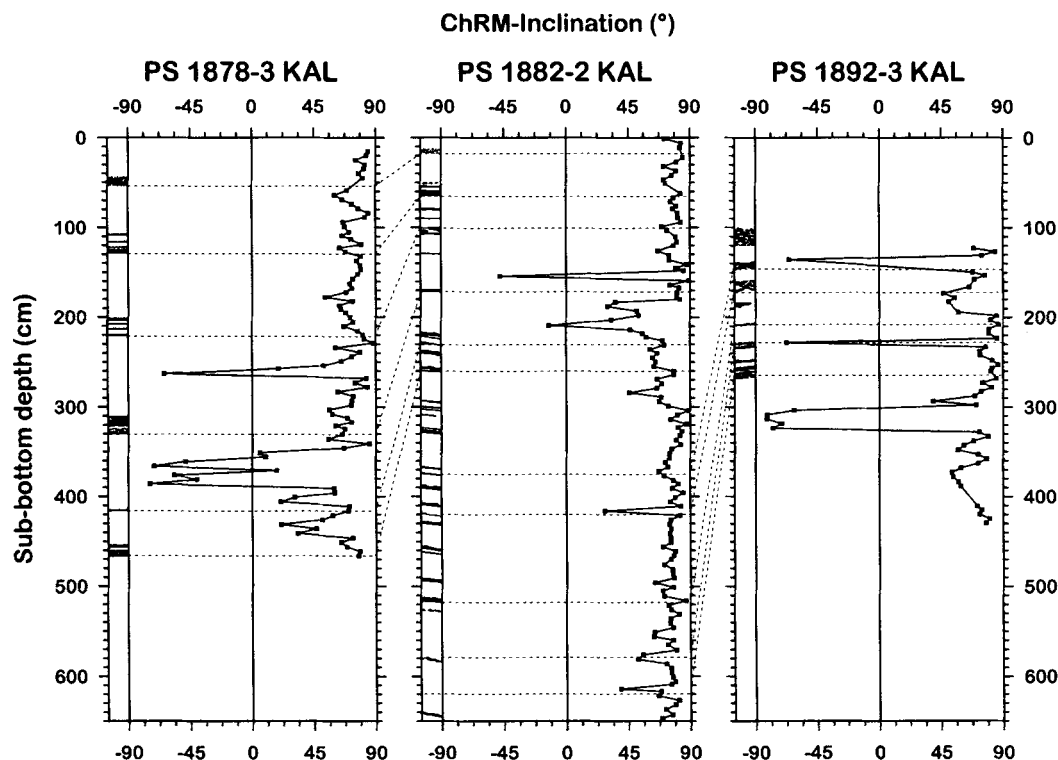


Figure 10. Sediment cores from the base of Vesteris Banken seamount, Greenland Sea: downcore variations of inclinations of the ChRM. Volcanic ash layers and correlations according to Figs 3, 4 and 5.

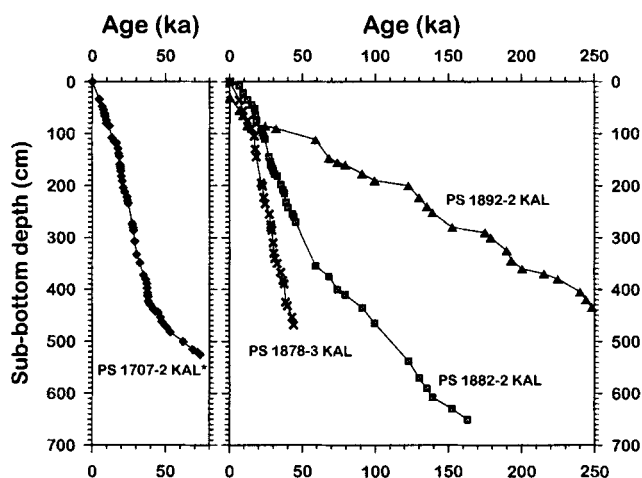


Figure 11. Age–depth plots of the cores from the Jan Mayen Fracture Zone (left) and Vesteris Banken (right).

(Nowaczyk 1997, this issue). With the correlation shown in Fig. 8 and the age model given in Table 3, the inclination swing at 280 cm in core PS 1707–2 KAL* may be interpreted as an incomplete record of the Mono Lake excursion and the excursion near the core base as part of the Norwegian–Greenland Sea event (Bleil & Gard 1989; Nowaczyk & Baumann 1992; Nowaczyk *et al.* 1994).

The Mono Lake event is also documented in core PS 1882–2 KAL at 150 cm (Fig. 9a). In this core the Laschamp event is documented only by some shallow inclinations (215–180 cm). A short excursion at 410 cm within the late stage 5 might be due to the Norwegian–Greenland Sea event. However, the

palaeomagnetic data from core PS 1882–2 KAL are of lower quality because numerous ash layers and a few thin turbidites are intercalated with the hemipelagic muds.

The magnetostratigraphic record of core PS 1892–3 KAL is shown in Fig. 9(b). The uppermost 60–70 cm of this core was slightly disturbed by the coring process and a hiatus can be recognized from stable-isotope analysis in the time span between oxygen isotope stages 1 and 3 (Fig. 4). Nevertheless, the magnetostratigraphic results below *c.* 100 cm document one pronounced geomagnetic event and two isolated samples, each with reversed inclinations. The polarity event from 325 to 300 cm exhibits directional variations similar to the Laschamp event, as recorded in cores PS 1878–3 KAL and PS 1707–2 KAL at roughly the same depth intervals. Correlation of this core with the other two cores from Vesteris Banken using high-resolution magnetic susceptibility (Fig. 3), stable-isotope data (Fig. 4) and biostratigraphic data (Fig. 5) assigns an early stage 6 age to this event, which can thus be identified as the Biwa I event (Kawai *et al.* 1972), also called the Jamaica event (Wollin *et al.* 1971). The single samples at 137 cm (near stage boundary 4/5) and 230 cm (stage boundary 5/6) exhibit demagnetization characteristics comparable with those of the samples displayed in Fig. 6 (a viscous normal overprint superimposed on a stable high-coercivity reversed ChRM direction). The 137 and 230 cm samples are related to the Norwegian–Greenland Sea event (Bleil & Gard 1989) and the Blake event (Smith & Foster 1969), respectively. Nevertheless, the data density here is again insufficient for a detailed analysis in terms of geomagnetic field variations. The ChRM inclination records of all three Vesteris Banken sediment cores shown in Fig. 10, together with the ash-layer pattern, again supports the correlation scheme according to Figs 3–5.

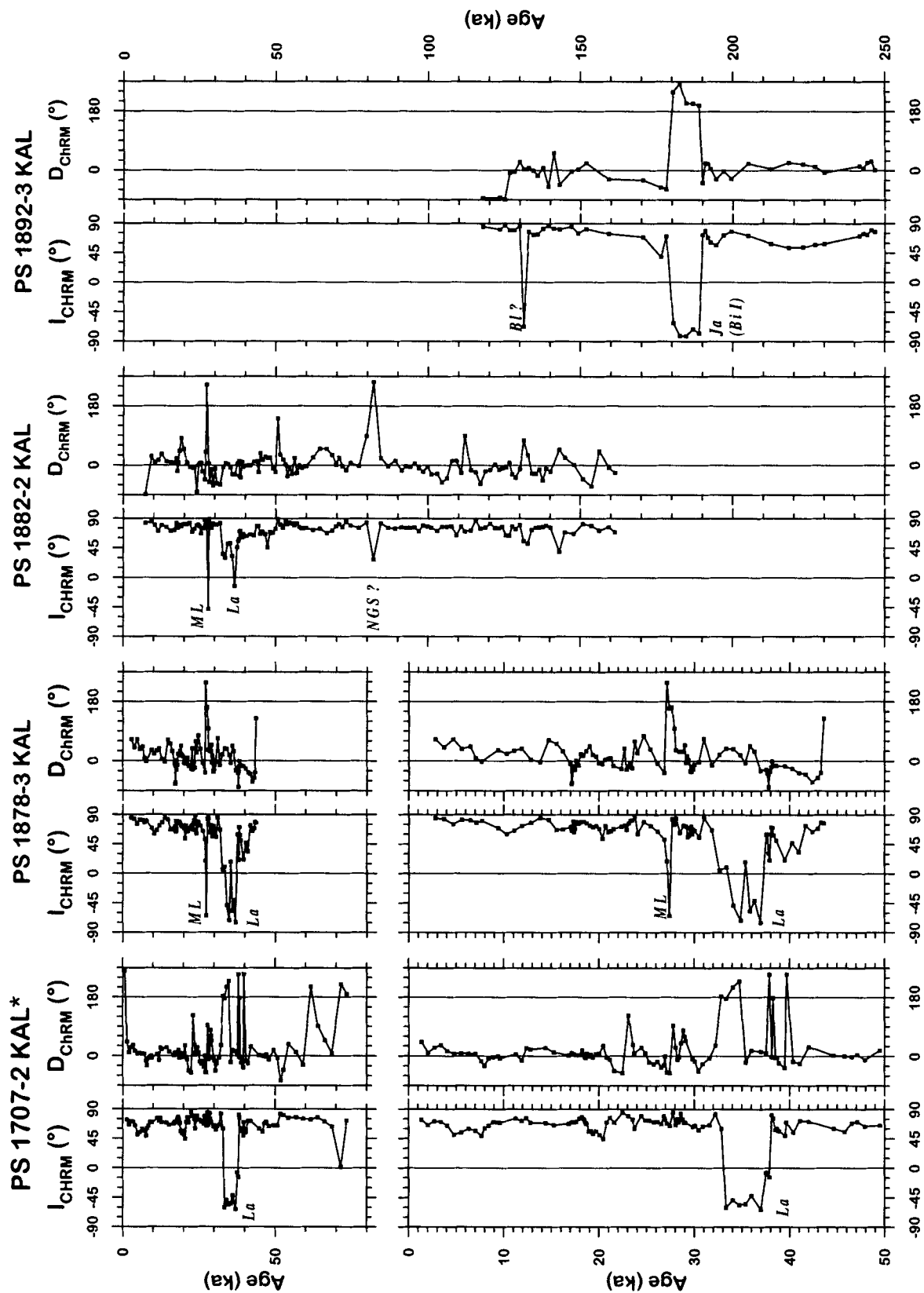


Figure 12. ChRM inclinations and declinations versus age of Greenland Sea sediments derived from sites PS 1707, 1878 1882, and 1892. Additional plots with stretched time axis are given for sites PS 1707 and 1878 on the lower left. The polarity events are labelled as follows: ML—Mono Lake; La—Laschamp; NGS—Norwegian–Greenland Sea; BI—Blake; Ja—Jamaica; Bi I—Biwa I.

Table 4. Updated list of referenced age ranges related to the Biwa I/Jamaica polarity event (see Nowaczyk *et al.* 1994).

#	Age range	Reference	Location
1	175–190	Wollin <i>et al.</i> (1971)	NW Pacific
2	176–186	Kawai <i>et al.</i> (1972)	Lake Biwa, Japan
3	200–215	Ryan (1972)	Mediterranean Sea
4	175–185	Bleil & Gard (1989)	Norwegian–Greenland Sea
5	160–180	Liddicoat (1990)	California, USA
6	171–181	Nowaczyk & Baumann (1992)	Fram Strait
7	180 < <i>t</i> < 218	Herrero-Bevera <i>et al.</i> (1994)	Oregon, USA
8	180–190	Negrini <i>et al.</i> (1994)	Oregon, USA
9	175–190	Weeks <i>et al.</i> (1995)	North Atlantic
10	156 ± 26	Peate <i>et al.</i> (1996)	New Mexico, USA
11	179–189	this study	Greenland Sea

DISCUSSION OF THE PALAEOMAGNETIC RECORD OF THE LAST 200 KA

The age models for the four cores discussed are displayed in Fig. 11. They were used to transform the magnetostatigraphic data into time-series, as displayed in Fig. 12. Ages between the data points given in Table 3 and Fig. 11 were interpolated linearly. Dating errors for AMS¹⁴C ages are of the order of 1 ka or less (Table 2). Errors in the assignment of oxygen isotope stage boundaries are of the order of 10 cm maximum, so that the total dating errors should be, depending on sedimentation rates, in the range 4 ka (2.5 cm ka⁻¹) to 2 ka (5 cm ka⁻¹).

Palaeomagnetic data for core PS 1892–3 KAL younger than 110 ka have been omitted because of the large directional scatter in its upper part. Additionally, due to different sedimentation rates at the four sites, the palaeomagnetic database is quite heterogeneous. The best data coverage is for the time interval back to about 60 ka (sites PS 1707, 1878 and 1882). Within this interval two geomagnetic events can be recognized: the Mono Lake excursion at 28–27 ka and the Laschamp event at 37–33 ka. The ages derived from the cores in this study are in good agreement with the age ranges for these

events summarized in Løvlie (1989) and Nowaczyk *et al.* (1994). Due to the variable positions of the real magnetic North pole and the high northern latitude of the core sites, the declinations show a large scatter. The Laschamp event exhibits a declination swing of about 180° only in core PS 1707–2 KAL, but because of the high latitude a field reversal can be recognized mainly from the inclination variation. In contrast, the Mono Lake excursion is recorded by declination and inclination only in two cores (sites PS 1878 and 1882). At site PS 1707 a declination swing of about 90° can be observed at the corresponding time interval without any anomaly in the inclination. The loss of the quite short Mono Lake excursion in this core might be explained by variable sedimentation rates, undetected short hiatuses and perhaps an insufficient sampling density.

Although confined to a total of only two samples, the intermediate direction at 80 ka in core PS 1882–2 KAL might be related to the event originally detected by Bleil & Gard (1989) in the Norwegian–Greenland Sea and later confirmed in the Weddell Sea (Grünig 1991), in the Fram Strait (Nowaczyk 1991; Nowaczyk & Baumann 1992), at the Yermak Plateau (Nowaczyk *et al.* 1994) and also in the loess/palaeosol sequence of China (Hongbo *et al.* 1995). A similar sparse result

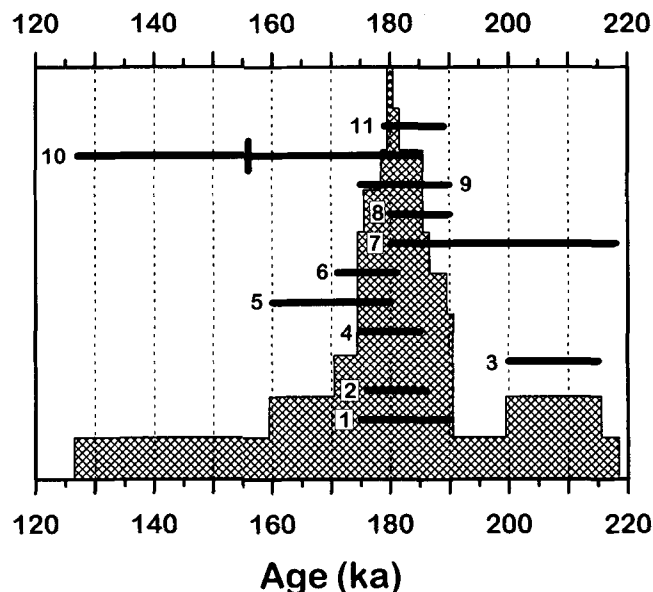


Figure 13. Age ranges published for the Biwa I/Jamaica polarity event according to references given in Table 4. The cross-hatched area was obtained by simply stacking the age ranges with a weighting of 1. The half-width thus results in an age range of 186–174 ka for this polarity event.

was obtained for the prominent Blake event (Smith & Foster 1969). Only the single sample at 131 ka in core PS 1892–3 KAL exhibits a reversed inclination that is close to the recently published age ranges of the Blake event of 128–118 ka (Yermak Plateau: Nowaczyk *et al.* 1994) and 130–110 ka (central China: Hongbo *et al.* 1995).

Only core PS 1892–3 KAL extends back to c. 250 ka. A pronounced polarity event documented in inclination and declination is recorded at 189–179 ka, which is early oxygen isotope stage 6. This event, identified as the Biwa I or Jamaica event, has been recorded at several sites worldwide (Table 4). The respective ages are displayed in Fig. 13. Simply giving each age range a weight of 1 and then stacking the intervals yields the cross-hatched area in Fig. 13. Even when ignoring the long age range given by Peate *et al.* (1996) this method suggests an age range of 186–174 ka for the Biwa I/Jamaica event.

CONCLUSIONS

A high-resolution magnetostratigraphic investigation performed on four sediment cores from the Greenland Sea yielded quite heterogeneous results, largely as a result of different sedimentary environments and varying deposition rates. Nevertheless, the overall results provide further evidence for three pronounced geomagnetic events: Mono Lake (28–27 ka), Laschamp (37–33 ka) and Biwa I/Jamaica (189–179 ka). Detailed correlation and dating of the cores is based on continuous high-resolution logs of magnetic susceptibility, stable-isotope stratigraphy, biostratigraphy and AMS¹⁴C data. The new results from 72.5°N and 73.5°N correspond to the geomagnetic event chronology spanning the latitude range from 69.5°N (Kolbeinsey Ridge: Bleil & Gard 1989), over 79°N (Fram Strait: Nowaczyk 1991; Nowaczyk & Baumann 1992) to 82°N (Yermak Plateau: Løvlie *et al.* 1986; Nowaczyk *et al.* 1994). From this study, together with studies from other regions, it is now obvious that the geomagnetic field did not continuously maintain a normal-polarity field configuration during the Brunhes Chron. Sediments from the Greenland Sea are mainly or even completely of lithogenic origin and are therefore characterized by high and stable NRM intensities. Bioturbation is very low or even absent. These properties might be one of the main reasons why these sediments are able to record high-frequency variations such as short polarity events that are not documented in many sediments from mid- to equatorial latitudes. Here, sediments often consist of a high percentage of biogenic material, bioturbation can be very intensive, and high contents of organic material might result in many (magnetically) destructive geochemical processes. Finally, only intense palaeo- and rock magnetic, as well as geochemical and sedimentological, studies all performed on numerous sediments from different sedimentary environments all over the globe will give the answer to the question why some types of sediments recorded geomagnetic polarity events in the Brunhes Chron and others did not.

ACKNOWLEDGMENTS

Profs U. Bleil (University of Bremen, Germany) and J. Thiede and Dr H.-J. Wallrabe-Adams (GEOMAR Kiel, Germany) encouraged this multidisciplinary work. G. Bonani performed AMS¹⁴C measurements at ETH Zurich, Switzerland, and

Dr H. Erlenkeuser (C-14 Lab of the Christian-Albrechts-University of Kiel, Germany) performed stable carbon and oxygen isotope measurements. The crews of R/V Polarstern are acknowledged for their technical support during cruises ARK V/3a and ARK VII/1. We thank L. Brück for assistance during sampling aboard R/V Polarstern and laboratory work in Bremen and V. Haase for his laboratory work in Freiberg. Dr T. McCann is acknowledged for improving the text of this manuscript. The Alfred-Wegener-Institut für Polar- und Meeresforschung provided ship time. This study was partly financed by the Bundesministerium für Forschung und Technologie and by the Deutsche Forschungsgemeinschaft through SFB 313.

REFERENCES

- Antonow, M., 1995. Sedimentationsmuster um den Vesteris Seamount (zentrale Grönlandsee) in den letzten 250.000 Jahren, *Dissertation*, University of Kiel, *GEOMAR Report*, **44**, Kiel.
- Bard, E., 1988. Correction of accelerator mass spectrometry ¹⁴C ages measured in planktonic foraminifera: Paleoceanographic implications, *Paleoceanography*, **3**, 635–645.
- Bard, E., Hamelin, B., Fairbanks, R.G. & Zindler, A., 1990. Calibration of the ¹⁴C timescale over the past 30.000 years using mass spectrometric U–Th ages from Barbados corals, *Nature*, **345**, 405–410.
- Bauch, H., 1993. Planktische Foraminiferen im Europäischen Nordmeer – ihre Bedeutung für die paläo-ozeanographische Interpretation während der letzten 600.000 Jahre, *Dissertation*, University of Kiel, *Ber. Sonderforschungsbereich 313*, **40**.
- Baumann, K.H., 1990. Veränderlichkeiten der Coccolithenflora des Europäischen Nordmeeres im Jungquartär, *Dissertation*, University of Kiel, *Ber. Sonderforschungsbereich 313*, **22**.
- Baumann, K.-H., Lackschewitz, K.S., Erlenkeuser, H., Henrich, R. & Jünger, B., 1993. Late Quaternary calcium carbonate sedimentation and terrigenous input along the east Greenland continental margin, *Mar. Geol.*, **114**, 13–36.
- Baumann, K.-H., Lackschewitz, K.S., Spielhagen, R.F. & Henrich, R., 1994. Reflection of continental ice sheets in late Quaternary sediments from the Nordic Seas, *Zbl. Geol. Paläont., Teil I* **7/8**, 897–912.
- Birgisdóttir, L., 1991. Die paläo-ozeanographische Entwicklung der Islandsee in den letzten 550.000 Jahren, *Dissertation*, University of Kiel, *Ber. Sonderforschungsbereich 313*, **34**.
- Bischof, J., 1990. Dropstones im Europäischen Nordmeer- Indikatoren für Meereströmungen in den letzten 300.000 Jahren, *Dissertation*, University of Kiel, *Ber. Sonderforschungsbereich 313*, **30**.
- Bleil, U. & Gard, G., 1989. Chronology and correlation of Quaternary magnetostratigraphy and nannofossil biostratigraphy in Norwegian-Greenland Sea sediments, *Geol. Rundschau*, **78**, 1173–1187.
- Bonhommet, N. & Babkine, J., 1967. Sur la présence d'aimantations inversées dans la Chaîne des Puys, *C. R. Acad. Sci. Paris*, **264**, 92–94.
- Craig, H., 1957. Isotopic standards for carbon and oxygen and correction factors for mass-spectrometric analysis of carbon dioxide, *Geochim. Cosmochim. Acta*, **12**, 1–133.
- Craig, H. & Gordon, L.I., 1965. Deuterium and oxygen-18 variations in the ocean and the marine atmosphere, in *Stable Isotopes in Oceanographic Studies and Paleotemperatures*, pp. 9–130, ed. Tongiorgi, E., Third SPOLETO conference on Nuclear Geology, Consiglio Nazionale della Ricerche, Laboratorio di Geologia Nucleare, Pisa.
- Denham, C.R. & Cox, A., 1971. Evidence that the Laschamp polarity event did not occur 13300–30400 years ago, *Earth planet. Sci. Lett.*, **13**, 181–190.
- Duplessy, J.-C., 1978. Isotope studies, in *Climatic Change*, pp. 46–67, ed. Gribbin, J., Cambridge University Press, Cambridge.

- Ganssen, G., 1983. Dokumentation von küstennahem Auftrieb anhand stabiler Isotope in rezenten Foraminiferen vor Nordwest-Afrika, *Meteor-Forsch. Ergebn.*, **37C**, 1–46.
- Gard, G., 1987. Late Quaternary calcareous nannofossil biostratigraphy and sedimentation patterns: Fram Strait, Arctica, *Paleoceanography*, **5**, 761–787.
- Gard, G., 1988. Late Quaternary calcareous nannofossil biochronology and paleo-oceanography of Arctic and Subarctic Seas, *Medd. Stockholms University of Geol. Inst.*, **275**, 1–45.
- Gard, G. & Backman, J., 1990. Synthesis of Arctic and Sub-Arctic coccolith biochronology and history of North Atlantic drift water influx during the last 500 000 years, in *Geological History of the Polar Oceans: Arctic vs. Antarctic*, pp. 417–436, eds. Bleil, U. & Thiede, J., Kluwer Academic Publishers, Dordrecht.
- Goldschmidt, P.M., 1994. The ice-rafting history in the Norwegian-Greenland Sea for the last two glacial/interglacial cycles, *Dissertation*, University of Kiel, *Ber. Sonderforschungsbereich 313*, **50**.
- Grünig, S., 1991. Quartäre Sedimentationsprozesse am Kontinentalhang des Süd-Orkney-Plateaus im nordwestlichen Weddellmeer, Antarktis (Quaternary sedimentation processes on the continental margin of the South Orkney Plateau, NW Weddell Sea, Antarctica), *Dissertation*, University of Bremen, *Rep. Polar Res.*, **75** (English abstract).
- Haase, K.M., Hartmann, M. & Wallrabe-Adams, H.-J., 1996. The geochemistry of ashes from Vesterisbanken seamount, Greenland Basin: implications for the evolution of an alkaline volcano, *J. Volc. Geotherm. Res.*, **70**, 1–19.
- Herrero-Bevera, E., Helsley, C.E., Sarna-Wojcicki, A.M., Lajoie, K.R., Meyer, C.E., McWilliams, M.O., Negrini, R.M., Turrin, B.D., Donnelly Nolan, J.M. & Liddicoat, J.C., 1994. Age and correlation of a paleomagnetic episode in the western United States by $^{40}\text{Ar}/^{39}\text{Ar}$ dating and tephrochronology: The Jamaica, Blake, or a new polarity episode? *J. geophys. Res.*, **99**, 24 091–24 103.
- Hogg, N.G., 1973. On the stratified TAYLOR column, *J. Fluid Mech.*, **58**, 517–537.
- Hongbo, Z., Rolph, T., Shaw, J. & Zhisheng, A., 1995. A detailed palaeomagnetic record for the last interglacial period, *Earth planet. Sci. Lett.*, **133**, 339–351.
- Imbrie, J., Hays, J.D., Martinson, D.G., McIntyre, A., Mix, A.C., Morley, J.J., Pisias, N.G., Prell, W.L. & Shackleton, N.J., 1984. The orbital theory of Pleistocene climate: support from a revised chronology of the marine $\delta^{18}\text{O}$ record, in *Milankovitch and Climate*, Part I, pp. 269–305, eds Berger, A.L. & Imbrie, J., Reidel, Dordrecht.
- Johannessen, O.M., 1986. Brief overview of the physical oceanography, in *The Nordic Seas*, pp. 103–127, ed. Hurdle, B.G., Springer, Berlin.
- Johnson, G.L. & Campsie, J., 1976. Morphology and structure of the western Jan Mayen Fracture Zone, *Norw. Polarinst. Arb.*, **1974**, 69–81.
- Jünger, B., 1994. Tiefenwassererneuerung in der Grönlandsee während der letzten 340.000 Jahre, *Dissertation*, University of Kiel, *GEOMAR Report*, **35**, 1–103.
- Kassens, H., Hubberten, H.-W., Pryamikov, S.M. & Stein, R., 1994. Russian-German cooperation in the Siberian shelf seas: Geo-system Laptev-Sea, *Rep. Polar Res.*, **144**.
- Kawai, N., Yaskawa, K., Nakajima, T., Torii, M. & Horie, S., 1972. Oscillating geomagnetic field with a recurring reversal discovered from Lake Biwa, *Proc. Japan Acad.*, **48**, 186–190.
- Kirschvink, J.L., 1980. The least-squares line and plane and the analysis of palaeomagnetic data, *Geophys. J. R. astr. Soc.*, **62**, 699–718.
- Kromer, B., Pfeleiderer, C., Schlosser, P., Levin, I., Münnich, K., Bonani, G., Suter, M. & Wölfli, W., 1987. AMS ^{14}C -measurements of small volume oceanic water samples: experimental procedure and comparison with low-level counting technique, *Nucl. Inst. Meth.*, **29**, 302–305.
- Liddicoat, J.C., 1990. Aborted reversal of the palaeomagnetic field in the Brunhes Normal Chron in east-central California, *Geophys. J. Int.*, **102**, 747–752.
- Løvlie, R., 1989. Palaeomagnetic excursions during the last interglacial/glacial cycle: a synthesis, *Quat. Int.*, **3/4**, 5–11.
- Løvlie, R., Markussen, B., Sejrup, H.P. & Thiede, J., 1986. Magnetostatigraphy in three Arctic Ocean sediment cores; arguments for geomagnetic excursions within oxygen-isotope stage 2–3, *Phys. Earth planet. Inter.*, **43**, 173–184.
- Martinson, D.G., Pisias, N.G., Hays, J.D., Imbrie, J., Moore, T.C. & Shackleton, N.J., 1987. Age dating and the orbital theory of the Ice Ages: Development of a high-resolution 0–300 000 years chronostratigraphy, *Quat. Res.*, **27**, 1–29.
- Nam, S.I., Stein, R., Grobe, H. & Hubberten, H., 1995. Late Quaternary glacial-interglacial changes in sediment composition at the East Greenland continental margin and their paleoceanographic implications, *Mar. Geol.*, **122**, 243–262.
- Negrini, R.M., Erbes, D.B., Robertes, A.P., Verosub, K.L., Sarna-Wojcicki, A.M. & Meyer, C.E., 1994. Repeating waveform initiated by a 180–190 ka geomagnetic excursion in western North America: implications for field behavior during polarity transitions and subsequent secular variation, *J. geophys. Res.*, **99**, 24 105–24 119.
- Nowaczyk, N.R., 1991. Hochauflösende Magnetostatigraphie spätquartärer Sedimente arktischer Meeresgebiete (High-resolution magnetostatigraphy of late-Quaternary Arctic marine sediments, engl. abstr.), *Dissertation*, University of Bremen, *Rep. Polar Res.*, **78**.
- Nowaczyk, N.R., 1997. High-resolution magnetostatigraphy of four sediment cores from the Greenland Sea—II. Rock magnetic and palaeointensity data, *Geophys. J. Int.*, **131**, 325–334 (this issue).
- Nowaczyk, N.R. & Baumann, M., 1992. Combined high-resolution magnetostatigraphy and nannofossil biostratigraphy for late Quaternary Arctic Ocean sediments, *Deep Sea Res.*, **39**, 567–601.
- Nowaczyk, N.R., Frederichs, T.W., Eisenhauer, A. & Gard, G., 1994. Magnetostatigraphic data from late Quaternary sediments from the Yermak Plateau, Arctic Ocean: evidence for four geomagnetic polarity events within the last 170 Ka of the Brunhes Chron, *Geophys. J. Int.*, **117**, 453–471.
- Peate, D.W., Chen, J.H., Wasserburg, G.J., Papanastassiou, D.A. & Geissman, J.W., 1996. ^{238}U – ^{230}Th dating of a geomagnetic excursion in Quaternary basalts of the Albuquerque Volcanoes Field, New Mexico (USA), *Geophys. Res. Lett.*, **23**, 2271–2274.
- Perry, R.K., Flemming, H.S., Weber, J.R., Kristoffersen, Y., Hall, J.K., Grantz, A., Johnson, G.L., Cherkis, N.Z. & Larsen, B., 1986. *Bathymetry of the Arctic Ocean*, Naval Research Laboratory, Acoustic Division, printed by the Geological Society of America.
- Roberts, D.J., Hogg, N.G., Bishop, D.G. & Flewellen, C.G., 1974. Sediment distribution around moated seamounts in the Rockall Trough, *Deep Sea Res.*, **21**, 175–184.
- Roden, G.I., 1987. Effects of seamounts and seamount chains on ocean circulation and thermohaline structure, in *Seamounts, Islands, and Atolls*, eds. Keating, B.H., Fryer, P., Batiza, R. & Boehlert, G.W., *Am. Geophys. Union*, **43**, 335–354, Washington, DC.
- Ryan, W.B.F., 1972. Stratigraphy of late Quaternary sediments in the Eastern Mediterranean, in *The Mediterranean Sea: A Natural Sedimentation Laboratory*, pp. 149–169, ed. Stanley, D.J., Dowden, Hutchinson & Ross, Inc., Stroudsburg, PA.
- Sarnthein, M., Jansen, E., Arnold, M., Duplessy, J.C., Erlenkeuser, H., Flatøy, A., Veum, T., Vogelsang, E. & Weinelt, M.S., 1992. $\delta^{18}\text{O}$ time-slice reconstruction of meltwater anomalies at termination I in the North Atlantic between 50 and 80°N, in *The Last Deglaciation: Absolute and Radiocarbon Chronologies*, pp. 183–200, eds. Bard, E. & Broecker, W.S., Springer Verlag, Berlin.
- Schiffelbein, P., 1986. The interpretation of stable isotopes in deep-sea sediments: an error analysis case study, *Mar. Geol.*, **70**, 313–320.
- Shackleton, N.J. & Opdyke, N.D., 1973. Oxygen isotope and paleomagnetic stratigraphy of Equatorial Pacific core V28–238: Oxygen isotope temperatures and ice volumes on a 105 year and 106 year scale, *Quat. Res.*, **3**, 39–55.
- Shackleton, N.J. & Opdyke, N.D., 1976. Oxygen isotope and paleomagnetic stratigraphy of Pacific core V28–238 Late Pliocene to Latest Pleistocene, *Mem. Geol. Soc. Am.*, **145**, 449–464.

- Spielhagen, R.F., 1991. Die Eisdrift in der Framstraße während der letzten 200.000 Jahre, *Dissertation*, University of Kiel, GEOMAR Report, 4.
- Smith, J.D. & Foster, J.H., 1969. Geomagnetic reversal in Brunhes normal polarity Epoch, *Science*, **163**, 565–567.
- Struck, U., 1992. Zur Paläo-Ökologie benthischer Foraminiferen im Europäischen Nordmeer während der letzten 600.000 Jahre, *Dissertation*, University of Kiel, *Ber. Sonderforschungsbereich 313*, 38.
- Thiede, J. & Hempel, G., eds., 1991. Die Expedn ARKTIS-VII/1 mit FS 'Polarstern' 1990, *Rep. Polar Res.*, **80**.
- Vogelsang, E., 1990. Paläo-Ozeanographie des Europäischen Nordmeeres an Hand stabiler Kohlenstoff- und Sauerstoffisotope, *Dissertation*, University of Kiel, *Ber. Sonderforschungsbereich 313*, 23.
- Vogt, P.R., 1986. Geophysical and geochemical signatures and plate tectonics, in *The Nordic Seas*, pp. 413–662, ed. Hurdle, B.G., Springer, Berlin.
- Weeks, R.J., Laj, C., Edignoux, L., Mazaud, A., Labeyrie, L., Roberts, A.P., Kissel, C & Blanchard, E., 1995. Normalized natural remanent magnetisation intensity during the last 240 000 years in piston cores from the central North Atlantic Ocean: geomagnetic field intensity or environmental signal?, *Phys. Earth planet. Inter.*, **87**, 213–229.
- Weinelt, M., 1993. Veränderungen der Oberflächenzirkulation im Europäischen Nordmeer während der letzten 60.000 Jahre – Hinweise aus stabilen Isotopen, *Dissertation*, University of Kiel, *Ber. Sonderforschungsbereich 313*, 41.
- Winn, K., Sarnthein, M. & Erlenkeuser, H., 1991. $\delta^{18}\text{O}$ stratigraphy and chronology of Kiel sediment cores from the East Atlantic, *Rep. Geol. Paläontol. Inst.*, University of Kiel.
- Wollenburg, I., 1993. Sedimenttransport durch das arktische Meereis: Die rezente lithogene und biogene Materialfracht. *Dissertation*, University of Kiel, *Rep. Polar Res.*, **127**.
- Wollin, G., Ericson, D.B., Ryan, W.B.F. & Foster, J.H., 1971. Magnetism of the earth and climatic changes, *Earth planet. Sci Lett.*, **12**, 175–183.